IET Microwaves, Antennas & Propagation

Research Article

IET Journals
The Institution of Engineering and Technology

Analysis of the radiowave propagation in an underground mine based on the modified Ray launching method

ISSN 1751-8725
Received on 2nd December 2014
Revised on 26th March 2015
Accepted on 7th April 2015
doi: 10.1049/iet-map.2014.0807
www.ietdl.org

Slawomir Kubal ✉, *Kamil Staniec, Ryszard J. Zieliński*

Department of Telecommunications and Teleinformatics, Wroclaw University of Technology, Wyb. Wyspianskiego 27, 50-370 Wroclaw, Poland

✉ *E-mail: slawomir.kubal@pwr.edu.pl*

Abstract: The study presents the developed model of electromagnetic wave scattering occurring on the irregular surfaces. This model was implemented in the Ray launching (RL) method. Based on the modified RL, the analysis of electromagnetic wave propagation in an underground mine was performed. The results of theoretical analyses were compared with the results of measurements (from a copper mine) to determine the degree improvement in the electromagnetic field prediction accuracy after the developed model application.

1 Introduction

An underground mine excavation is a specific example of a real, indoor propagation environment. This environment is usually created by a system of corridors with a relatively regular cross-section. However, the walls have a considerable degree of irregularities. Owing to significant irregularities of the walls, it is a very complex environment in terms of propagation analysis. Despite this, wireless systems are increasingly used in this environment, not only to provide connectivity and voice transmission, but also to control the mining facilities or to locate workers and equipment. Planning procedures for all wireless systems require a detailed analysis of propagation. For this purpose, it is necessary to develop propagation models that could be used to predict the electromagnetic field strength as accurately as necessary for the purpose of planning a wireless systems. Methods based on geometrical optics (GO) are very often used for propagation analysis in the indoor environment because of their high conformance with the measurement results in a simple (office) [1, 2] or a more complicated environment [3, 4], also in combination with the analysis of diffraction at the edges according to the uniform theory of diffraction (UTD) [5]. Attempts to use GO-based methods in tunnels, including those with irregular walls, are presented, for example in [6–10].

Early works about the analysis of radio wave propagation in the mine environment already appeared in the seventies of the last century. Emslie in his work [11] proposes to replace the mine corridor with a waveguide, and then calculates the propagation attenuation according to the waveguide techniques, taking into account only the basic modes. He also develops the scattering model for the lower frequency of UHF band taking into account the irregularities of the walls, referring to simple rectangular corridors. The Ray launching (RL) method used for the calculation of propagation in mine workings is presented in [12]. The authors, based on measurement results, introduce additional propagation attenuation resulting from irregularities of the walls, encountered in a realistic underground environment. The RL method used to analyse the field distribution in the mine corridors is also described in [13]. In this paper the author proposes a random change in the direction of specular reflections in the case of wave incidence on an irregular surface. The ray tracing (RT) method is used for the propagation analysis in a mine by authors of [14, 15]. However, in [15], the authors focus only on corridors with a semi-elliptical cross-section in which there are no walls irregularities. In [14], the authors propose to use the RT method in combination with the image method in corridors with rectangular vertical cross-section and varying horizontal cross-section. Based on the basic modes waveguide method, developed by Emslie, the authors of [16] develope a model for the corridors with a rectangular cross-section, based on a multimode approach. Then, based on the developed model, they confirm that increasing the walls irregularity increases the attenuation resulting from the scattering of electromagnetic waves. In [17] the application of Kirchoff approximation for the calculation of propagation in mine environments was presented and to assess the impact of irregularities on the electromagnetic field distribution in the corridors of mine. The authors of [18–21] present a comparison of currently used methods for the analysis of field distribution in the mine environment: from the waveguide approach and by the approximation method finely to the full-wave methods. They determine their strengths and weaknesses, such as the complexity of the method, the computation time, the extent of phenomena taken into account and the range of applications, when used in this specific and complex environment.

In this paper a modified RL method was presented. The proposed model, in its basic version, is a pure realisation of the three-dimensional (3D) RL method, in that it allows discrete radiowave rays to be launched (following discretised antenna radiation patterns as shown in Fig. 6) and tracked as they traverse the environment by way of multiple reflections determined by angle- and material-dependent reflection coefficients. As an outcome, an exact channel impulse response as well as angle-of-arrival characteristics (in E- and H-plane) can be obtained not just at the reception point but also at up to 450 other predefined points located throughout the propagation area. Although the latter option is already quite distinguishing in comparison with 'state of the art' simulation tools (selected out of the most renowned products, such as those of Siradel [22] or Awe Communication's Proman [23]), the additional feature outperforming existing models of this kind has been provided by incorporating a measurement-based statistical model of the walls irregularities. This inclusion, as will be shown later, has led to the formulation of quite novel conclusions regarding the sensitivity of LOS and NLOS propagation to the irregular wall surfaces inside mines.

The paper presents the results of calculations in which the field strength of each ray at each reflection was multiplied by an additional factor (determined on the basis of the developed scattering models) depending on the irregularities of the walls. These new models were developed using methods based on GO

and they take into account the basic parameters of walls irregularities. Theoretical results were compared with measurement results performed in a real underground copper mine.

2 Electromagnetic wave scattering

The scattering of electromagnetic waves occurs during the wave incidence on an irregular, uneven surface. This causes the wave incident on an irregular surface to be partially reflected in the direction of specular reflection and partially scattered in other directions. During the propagation of electromagnetic waves over a flat surface, the direct and reflected waves reach the receiver. However, if the wave propagates over an irregular surface, the former contributions (i.e. direct and reflected) are assisted by one more phenomenon, namely the scattering. The scattering analysis is complicated and time-consuming. Therefore it was necessary to develop criteria for surface irregularities. These criteria are used to estimate whether a particular surface can be considered as flat or not. In the latter case it is necessary to analyse the scattering occurring on the irregularities. The basic criterion was proposed by Rayleigh, according to which, if the phase difference of two reflected from the surface rays exceeds the value of $\pi/2$, the surface is considered as irregular [24]. This criterion specifies the maximum value of irregularities height, for which the surface can be regarded as flat, at the same time determining the minimum value of this parameter, for which the surface is considered to be irregular. The Rayleigh criterion can be written as function of the standard deviation of irregularities σ_h in relation to the wavelength λ (1)

$$f\left(\frac{\sigma_h}{\lambda}\right) = \frac{1}{8 \cdot (\sigma_h/\lambda) \cdot \cos\theta} \leq 1 \quad (1)$$

where, σ_h – standard deviation of irregularities height, λ – wavelength, θ – angle of wave incidence (measured with respect to the normal vector of the plane).

Fig. 1 shows the Rayleigh criterion, plotted according to (1) for four different, exemplary values of the σ_h/λ parameter. Based on this figure it can be seen that for incidence angles for which the curve plotted for a particular value of the σ_h/λ, lies below the line with the value 1, the surface is considered as an irregular. It could be noted that even for the value of $\sigma_h/\lambda = 0.25$ (low roughness compared with the wavelength), the surface having such properties is considered to be irregular for incident angles lower than approx. 60°.

The above-mentioned standard deviation of irregularity heights is the primary parameter of a random irregular surface. The second important parameter describing the properties of such surfaces is the correlation length 'l', determined as a value for which the autocorrelation function of the irregularities is equal to 1/e [24]. The autocorrelation function (and thus the correlation length) determines the rate of irregularities variability when moving along its length (width). The higher value of the correlation length, the lower the change in the surface roughness along its length.

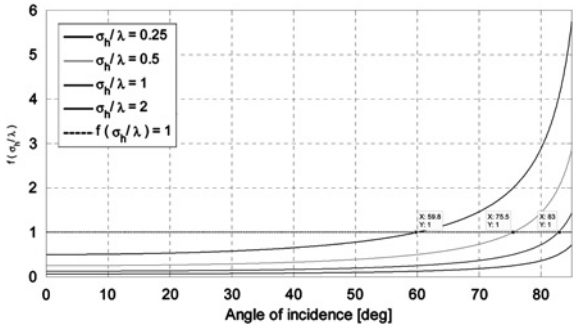

Fig. 1 *Rayleigh criteria for different value of σ_h/λ*

3 Scattering models for specular direction

During the electromagnetic wave incidence on an irregular surface there are a number of phenomena that directly affect the direction and amplitude of the scattered wave. Parameters of the wave reflected from such a surface are very different from the parameters of the wave reflected from the flat surface (assuming that the same ray beam illuminates both surfaces at the same angle). Such a situation in which beam with a particular width radiated from Tx point falls on the two different types of surfaces is shown in Fig. 2.

To compare the above-mentioned cases, it is necessary to calculate the field strength at specific points in Rx (the same for flat and irregular surfaces). For a flat surface, only two rays: the direct and the reflected can reach to a particular point Rx, hence the total field strength at this point can be written as

$$E_{total} = E_{LOS} + E_r \quad (2)$$

where, E_{LOS} – electric field strength of the direct ray [V/m], E_r – electric field strength of the reflected ray [V/m].

Equation (2) is often used for the calculation of electromagnetic wave propagation over a flat surface and is the basis for the popular two-ray model. The situation is different if the same electromagnetic wave impinges on an irregular surface. In this case, a much higher number of rays can reach a particular Rx point. The wave incident on an irregular surface can be reflected (single or multiple), diffracted or both reflected and diffracted. The number of rays that reach the point Rx, depends on the surface properties. The total value of the field strength $\boldsymbol{E}_{total}$ can be written as (3)

$$E_{total} = E_{LOS} + \sum E_r + \sum E_d + \sum E_{rn} + \sum E_{dr} \quad (3)$$

where, E_d – electric field strength of the diffracted ray [V/m], E_{rn} – electric field strength of the multiple reflected ray [V/m], E_{dr} – electric field strength of the diffracted and reflected (or reflected and diffracted) ray [V/m].

As for the flat surface, the direct component is independent of the surface properties. Therefore this component has been omitted for the analysis of the phenomena occurring at the wave incidence on the irregular surface. The total electric field at the point Rx, which occurs as a result of wave incidence on an uneven surface can be written as

$$E = \sum E_r + \sum E_d + \sum E_{rn} + \sum E_{dr} \quad (4)$$

The field strength of reflected ray has been calculated according to methods based on GO (RT and image method), while the diffracted rays have been analysed according to the UTD.

To analyse the impact of surface parameters on the wave scattering, a number of studies for different cases were performed. A general simulation scenario is shown in Fig. 3 (β – the ray beam width, θ_i – the incidence angle relative to the normal vector). Tests were carried out for the surface with a length of 15 m and a width of 2 m. The source of electromagnetic waves was placed at a height of 2 m above the surface and at a distance of 5 m from the left edge. A beam of uniformly distributed rays was emitted from the source at a predetermined angle of incidence θ_i calculated relative to the normal vector of the flat surface. The electric field strength was calculated according to (5) at points arranged on the circumference of a circle with a particular radius R.

Analyses were performed for two types of irregular surface models. One with the rectangular grid model called two-dimensional (2D) model, whereas the other with triangular grid called a 3D model (shown in Fig. 2). Figs. 2*c* and *d* are representative examples of the surface models. Dimension of both surfaces is 2 × 5 metres. Both surfaces were generated with a mean value of irregularities $\mu_h = 0$ m, a standard deviation of irregularities $\sigma_h = 0{,}05$ m and with mean value of approximating

IET Microw. Antennas Propag., 2015, Vol. 9, Iss. 12, pp. 1241–1248

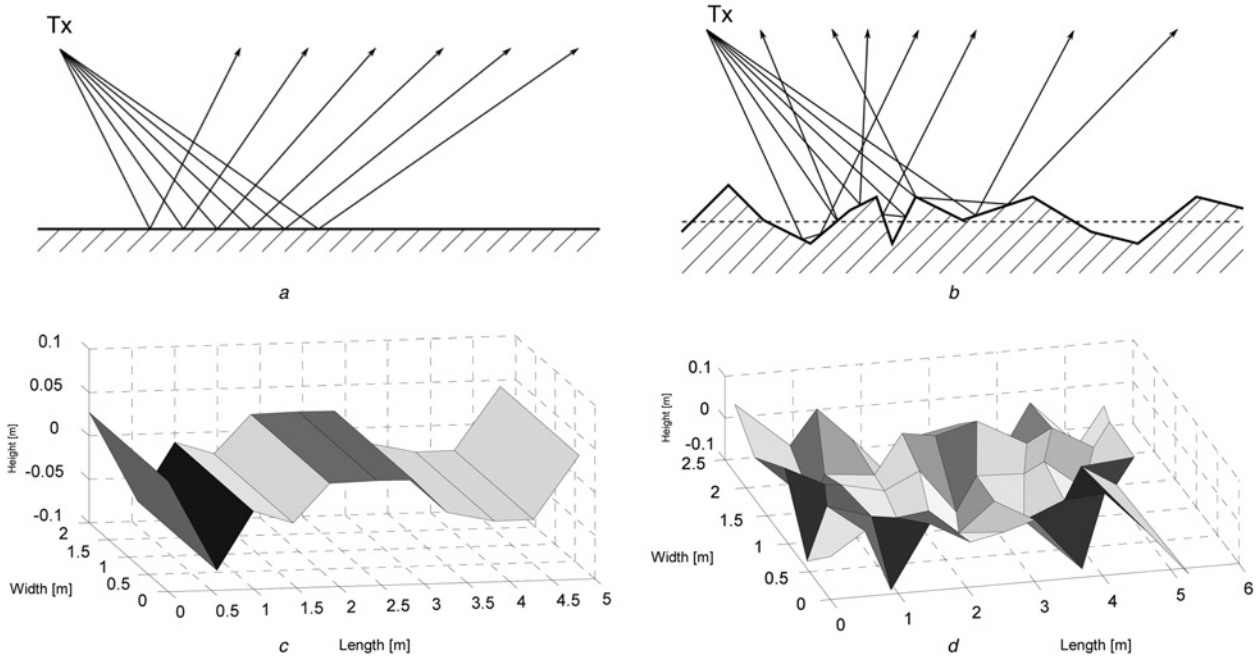

Fig. 2 *Reflecting of an electromagnetic wave from surface:*

a Flat
b Irregular and irregular surface models:
c 2D
d 3D

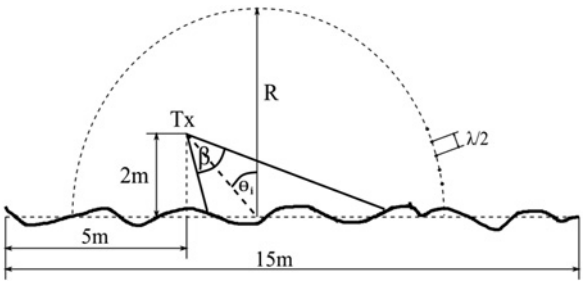

Fig. 3 *Simulation scenario*

plane length $\mu_L = 0{,}5$ m and standard deviation of approximating plane length $\sigma_L = 0{,}1$ m. A detailed description of these models is presented in [25]. Owing to the pseudo-random values of the surface parameters, all simulations were performed for 100 iterations and then the average value of electric field strength at particular points was calculated.

3.1 Model of scattering of an electromagnetic wave for the direction of specular reflection for the 2D model

The RL method determines ray propagation paths based on Snell's law. Therefore it was decided to develop a model, which describes the scattered field intensity in the specular direction, taking into account the parameters of the irregular surface, such as the standard deviation of irregularities height, the correlation length, the relative permittivity, the conductivity and the incidence angle of the wave on the irregular surface and its frequency. In the developed models the scattered wave field strength E_s was related to the field strength E_{flat} obtained for a flat surface with the same electrical parameters. Therefore these models could be directly used in the RL as a modification of the reflection coefficient. The mathematical models were developed using a multiple linear regression. In general, the regression is used to determine the relationship between the dependent variable Y and independent variables X. The main element of the regression model is a regression function, which analytically describes the above relationship. The regression model requires that the observations of the dependent variable Y are made at the set values of the independent variable X. This means that the random sample used in the construction of the model is defined by the number of observations 'n'. Hence, multiple linear regression model can be described by the relation [26]

$$Y_i = \beta_1 x_{i1} + \beta_2 x_{i2} + \cdots + \beta_k x_{ik} + \beta_{k+1} + \epsilon_1, \quad dla\, i = 1, 2, \ldots, n \tag{5}$$

where, ε_1 – model error, $x_{i1}, x_{i2}, \ldots, x_{ik}$ – a system implementation of the independent variable X, $\beta_1, \beta_2, \ldots, \beta_k$ – coefficients of multiple linear regression, β_{k+1} – a value of the regression constant.

The multiple linear regression model, described by relationship (5), could be written using a matrix notation

$$\boldsymbol{Y} = \boldsymbol{X}\boldsymbol{\beta} + \boldsymbol{\varepsilon} \tag{6}$$

where, $\boldsymbol{Y}$ – observation vector of the dependent variable with dimension $(n \times 1)$, $\boldsymbol{X}$ – observation vector of the independent variables with dimension $(n \times (k+1))$, $\boldsymbol{\beta}$ – vector of the regression coefficients with dimension $((k+1) \times 1)$, $\boldsymbol{\varepsilon}$ – vector of the model errors with dimension $(n \times 1)$.

To estimate the coefficients of the regression model it is necessary to minimise the relationship $\boldsymbol{S} = \boldsymbol{\varepsilon}^T\boldsymbol{\varepsilon}$ using the least squares method. Hence the vector of the coefficient's estimators $\hat{\boldsymbol{\beta}}$ could be written as

$$\hat{\boldsymbol{\beta}} = (\boldsymbol{X}^T\boldsymbol{X})^{-1}\boldsymbol{X}^T\boldsymbol{Y} \tag{7}$$

After determination of the $\hat{\boldsymbol{\beta}}$ vector, statistical significance of the each estimator is verified, using t-student and F-Snedecor distribution and the degree of compliance with the regression model is checked. During research for the developed scattering model, after checking dozens of the regression functions, variables

dependent and independent were selected experimentally as

$$\mathrm{Y} = \ln\left(\frac{E_\mathrm{s}(\theta_i)}{E_\mathrm{flat}(\theta_i)}\right); \quad X_1 = \sqrt{\frac{\sigma_\mathrm{h}}{\lambda}}; \quad X_2 = \ln\left(\frac{l}{\lambda}\right); \quad X_3 = \frac{\tan^2(\theta_i)}{\varepsilon_\mathrm{r}}; \quad X_4 = \sigma \tag{8}$$

where, $E_\mathrm{s}(\theta_i)$ – field intensity of scattered wave [V/m], $E_\mathrm{flat}(\theta_i)$ – field intensity of wave reflected from flat surface [V/m], l – correlation length [m], σ_h – standard deviation of irregularities height [m], λ – wavelength [m], θ_i – incidence angle [rad], ε_r – relative surface permittivity, σ – surface conductivity [S/m].

The scattered wave field intensity depends on the polarisation, therefore two separate models for the two polarisation types, parallel and perpendicular to the plane of incidence, were developed. The developed mathematical model of the scattered wave field intensity related to the field intensity of the wave reflected from a flat surface to the parallel polarisation takes a form (9)

$$\frac{E_\mathrm{s}(\theta_i)}{E_\mathrm{flat}(\theta_i)} = \left(\frac{l}{\lambda}\right)^{0,19} \cdot \mathrm{e}^{\left(-0,66\sqrt{\sigma_\mathrm{h}/\lambda}+2,24(\tan^2(\theta_i)/\varepsilon_\mathrm{r})+0,05\cdot\sigma-0,01\right)} \tag{9}$$

The developed model for an electromagnetic wave polarised perpendicular to the plane of incidence takes the form

$$\frac{E_\mathrm{s}(\theta_i)}{E_\mathrm{flat}(\theta_i)} = \left(\frac{l}{\lambda}\right)^{0,26} \cdot \mathrm{e}^{\left(-0,80\sqrt{\sigma_\mathrm{h}/\lambda}+0,31(\tan^2(\theta_i)/\varepsilon_\mathrm{r})+0,06\cdot\sigma-0,03\right)} \tag{10}$$

The proposed electromagnetic wave scattering model in the specular direction is designed for incidence angles less than 70°. It should be noted, that for some values of the incidence angle (depending on the surface parameters) calculated values could be greater than unity. This effect is particularly notable for parallel polarisation, for which the value of E_flat decreases for incidence angles near to the Brewster angle. The value of this angle for materials with relative dielectric permittivity comprised between approx. 7 to approx. 25 is in the range, respectively, from approx. 70° to approx. 80°. The value of ratio $E_\mathrm{s}/E_\mathrm{flat}$ >1 in the specular direction is possible, however it should be noted that in such cases for other directions this ratio is much smaller than unity, hence the law of energy conservation was satisfied. Taking into account the values greater than unity for the specular direction omitting other directions, may cause significant errors in calculation. Therefore threshold angles were determined for which it is possible to use the proposed model. If the calculated value of threshold angle $\theta_{i\mathrm{th}}$ is >70°, this threshold angle is set as 70° (as was written above it is the maximum value of the incidence angle for which the model was developed). The value of the threshold angle for the parallel polarisation is given by (11).

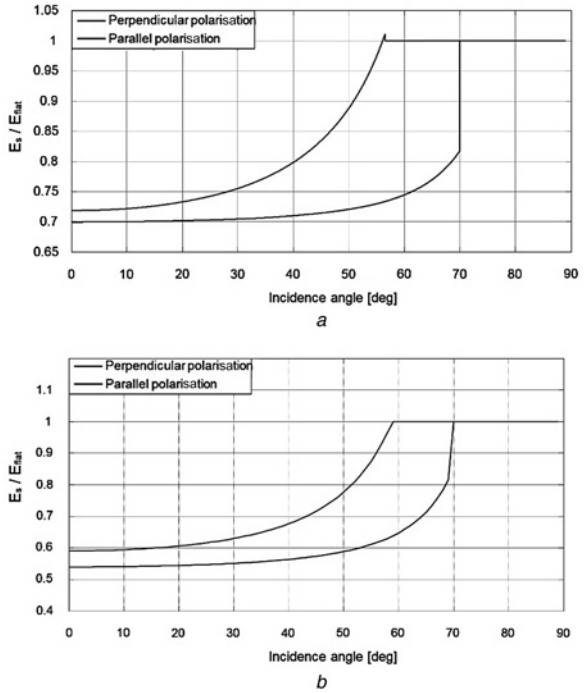

Fig. 4 *Example of results of developed scattering model for the surface models:*

a 2D
b 3D

$$\theta_{i\mathrm{th}} = \min\left(\arctan\left(\sqrt{\varepsilon_\mathrm{r}}\left(0,29\sqrt{\frac{\sigma_\mathrm{h}}{\lambda}} - 0,08\ln\left(\frac{l}{\lambda}\right) - 0,02\sigma + 0,004\right)\right), 70^\circ\right) \tag{11}$$

Whereas for the perpendicular polarisation it is given by (12)

$$\theta_{i\mathrm{th}} = \min\left(\arctan\left(\sqrt{\varepsilon_\mathrm{r}}\left(2,58\sqrt{\frac{\sigma_\mathrm{h}}{\lambda}} - 0,84\ln\left(\frac{l}{\lambda}\right) - 0,19\sigma + 0,1\right)\right), 70^\circ\right) \tag{12}$$

For incidence angle greater than $\theta_{i\mathrm{th}}$ it should be assumed $E_\mathrm{s}/E_\mathrm{flat} = 1$. This assumption was based on the Rayleigh criterion, according to which for larger values of the incidence angles, irregularities are becoming less important and the effect of electromagnetic wave scattering decreases. Fig. 4*a* shows examples of curves generated with regard to the threshold angle for the surface with parameters: $L = 1$ m, $\sigma_\mathrm{h} = 0.15$ m, $\varepsilon_\mathrm{r} = 15$, $\sigma = 0{,}15$ S/m and $f = 2.4$ GHz.

It should be also noted that the assumptions of GO are satisfied when the reflective surface dimensions are larger than the wavelength. The surface size is directly related to the correlation length, hence for the developed model this was assumed to be $(l/\lambda)_\mathrm{min} = 2$. In addition, the model can be used only for a surface, which irregularities satisfy the Rayleigh criterion. The model also has a lower limit frequency. All simulations, which were used to develop the models, were performed to frequencies >900 MHz. In addition (9) and (10) have a local maximum (in a frequency domain), which is equal to lower limit frequency and for 2D models this minimum usable frequency is equal to 800 MHz.

3.2 Model of scattering of an electromagnetic wave for the direction of specular reflection for the 3D model

Equations (13) and (14) are analogous to (9) and (10). They were prepared in the same way as (9) and (10), however for 3D surface model. Likewise, all assumptions and symbols are the same as for the equations obtained for 2D model. Owing to the fact that they were designed for a different surface model, they have different function coefficients, values of their border angles as well as the range of applicability. The scattered model for 3D surface model for parallel polarisation was also developed using multiple linear regression. This model takes the form (13)

$$\frac{E_\mathrm{s}(\theta_i)}{E_\mathrm{flat}(\theta_i)} = \left(\frac{l}{\lambda}\right)^{0,37} \cdot \mathrm{e}^{\left(-0,87\sqrt{(\sigma_\mathrm{h}/\lambda)}+2,9(\tan^2(\theta_i)/\varepsilon_\mathrm{r})+0,11\cdot\sigma-0,36\right)} \tag{13}$$

For the perpendicular polarisation (14)

$$\frac{E_\mathrm{s}(\theta_i)}{E_\mathrm{flat}(\theta_i)} = \left(\frac{l}{\lambda}\right)^{0,5} \cdot \mathrm{e}^{\left(-1,22\sqrt{(\sigma_\mathrm{h}/\lambda)}+0,91(\tan^2(\theta_i)/\varepsilon_\mathrm{r})+0,07\cdot\sigma-0,33\right)} \tag{14}$$

The value of threshold for the incidence angle for parallel

IET Microw. Antennas Propag., 2015, Vol. 9, Iss. 12, pp. 1241–1248

polarisation is described by (15)

$$\theta_{i\text{th}} = \min\left(\arctan\left(\sqrt{\varepsilon_\text{r}}\left(0,3\sqrt{\frac{\sigma_\text{h}}{\lambda}} - 0,13\ln\left(\frac{l}{\lambda}\right) - 0,04\sigma + 0,12\right)\right), 70^\circ\right) \quad (15)$$

For the perpendicular polarisation (16)

$$\theta_{i\text{th}} = \min\left(\arctan\left(\sqrt{\varepsilon_\text{r}}\left(1,34\sqrt{\frac{\sigma_\text{h}}{\lambda}} - 0,55\ln\left(\frac{l}{\lambda}\right) - 0,08\sigma + 0,36\right)\right), 70^\circ\right) \quad (16)$$

Moreover for these models the assumption that for incidence angles greater than $\theta_{i\text{th}}$ the ratio $E_\text{s}/E_\text{flat} = 1$ is valid. Fig. 4*b* shows the examples of curves generated with regard to the threshold angle for the surface with parameters: $l = 1$ m, $\sigma_\text{h} = 0.15$ m, $\varepsilon_\text{r} = 15$, $\sigma = 0{,}15$ S/m and $f = 2.4$ GHz.

For the scattering model for 3D surface model the condition concerned with minimum ratio of the correlation length to the wavelength, which takes a value equal to 2, is also valid. As for 2D models all simulations were performed to frequencies >900 MHz and (13) and (14) have the local maximum. For 3D models it was impossible to find other values of function parameters, that this local maximum had lower frequency and developed model had good accordance with simulations results. Therefore the frequency limit for these models is equal to 1,3 GHz.

4 Model validation

To determine the degree of increasing the prediction accuracy of the electromagnetic field distribution in the mine environment appropriate propagation measurements were carried out. All measurements were performed in the copper mine in Lubin (Poland), owned by KGHM Polish Copper SA. A typical excavation area (resembling a grid) was selected, located about 650 m below the surface. The measurement environment was treated by system of corridors with a regular structure, consisting of a rectangular stone blocks with dimensions of approx. 45 to 23 metres. The corridors in the mine had an average width of approx. 5 m and a height of approx. 3 m. Corridors are created by blowing up the rock, which is why their walls exhibit a considerable degree of irregularity. Examples of walls irregularities in the copper mine, where measurements were carried out, was shown in Fig. 5.

The irregularity parameters of a real mine wall were determined on the basis of the measured morphology for the 30 m section of the corridor wall, which are

- standard deviation of irregularities height $\sigma_\text{h} \simeq 0.15$ m,
- correlation length $l \simeq 2$ m.

These parameters are used in the simulations, of which the results are shown later in this paper. It is worth noting that the Kolmogorov–Smirnov and the Shapiro–Wilk test performed at a significance level of 0.05 gave a positive result, hence the irregularities have a normal distribution. Unfortunately, authors were unable to measure the electrical parameters of the rock from the Lubin mine. Therefore these values were assumed as the limestone ($\varepsilon_\text{r} = 7.5$ and $\sigma = 0.03$ S/m) [27]. Moreover it should be noted that there is significant humidity in the mine, which could have a pronounced impact on the electrical characteristics of materials, changing their reflective properties [28]. However the humidity impact on these parameters has not been taken into account in simulations.

For the calculated for galleries value $\sigma_\text{h} \simeq 0.15$ m and for measuring frequency 915, 1510 and 2440 MHz the ratio σ_h/λ amounts to 0.45, 075 and 1.22. For such values the popular

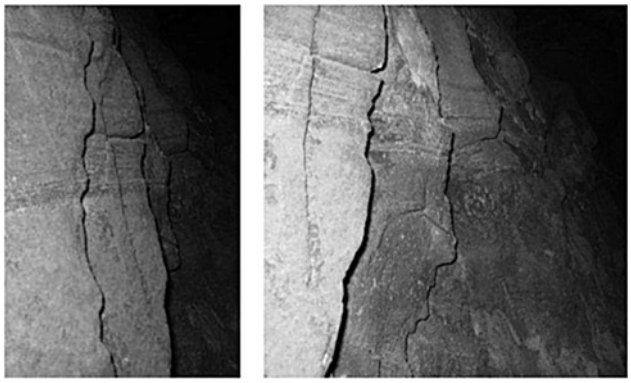

Fig. 5 *Irregularities of mine walls*

Rayleigh approximation [29], which also applies in the specular direction (as developed model) yields the zero value for most incidence angles. Hence, in accordance with this approximation, the wave is not reflected from the surface possessing such parameters. Based on the measurement results (presented later in the article) it is not a true statement. It should also be noted that this approximation takes into account only the standard deviation of the irregularities, not including the additional, equally important parameters such as the correlation length or their electrical parameters. As one can see, this approximation is very limited in use, which makes the developed original model functionally superior to the approximation.

A signal generator HAMEG HM8135 and an antenna Rohde & Schwarz HE300 (gain 17 dB) were used as a wave transmitter, while a spectrum analyzer Tektronix Hawk H600 and antenna Aaronia HyperLOG 6080 (gain 6 dB) were used to receive scattered waves. Tests were conducted for the three frequency bands 915 MHz, 1.51 GHz and 2.44 GHz. These three bands were selected because, besides the propagation measurement, also the performance tests of three wireless systems operating in these bands were conducted in the mine. Fig. 6 presents the signal transmitter located in the mine corridor and radiation characteristics of the transmitting antenna.

Measurements were performed in the main corridor and in transverse galleries extending from the main one, to determine the amount of energy penetrating these galleries. A detailed arrangement of the measuring points in the main corridor was shown in Fig. 7. The points have been chosen so that measurements were performed in the middle of each section and at the galleries intersection. Measurements were made, at each point, in the central part of the corridor at a height of approx. 1.5 m. Fig. 7 also shows the mine model designed to compare the measurement results with the simulation results, the latter performed in two scenarios: with and without the scattering. Fig. 7 also presents the location of the transmitter, and the direction of measurement for LOS conditions and transverse galleries numbers, in which propagation measurements were performed for the NLOS conditions. Measurements for all the transverse corridors (for NLOS conditions) were performed in the middle of each section and at the corridors intersection.

A comparative analysis was carried out using the RL method. An application developed by one of the authors was used to calculate the electromagnetic field distribution in the mine. The developed scattering models were implemented in this application, which made it to compare the results of measurements with the results of calculations. It should be noted that the application used for verification is based on the pure RL method which does not take into account the diffraction at the edges (refer to the fourth paragraph of Section 1 for a respective note on the applied model and a propagation mechanisms used therein, some helpful information can also be found in [13]).

Fig. 9 shows the comparative results of theoretical calculations (curves green, red and blue) and the results of measurements (black dots) for the sample measurement frequency of 2.4 GHz.

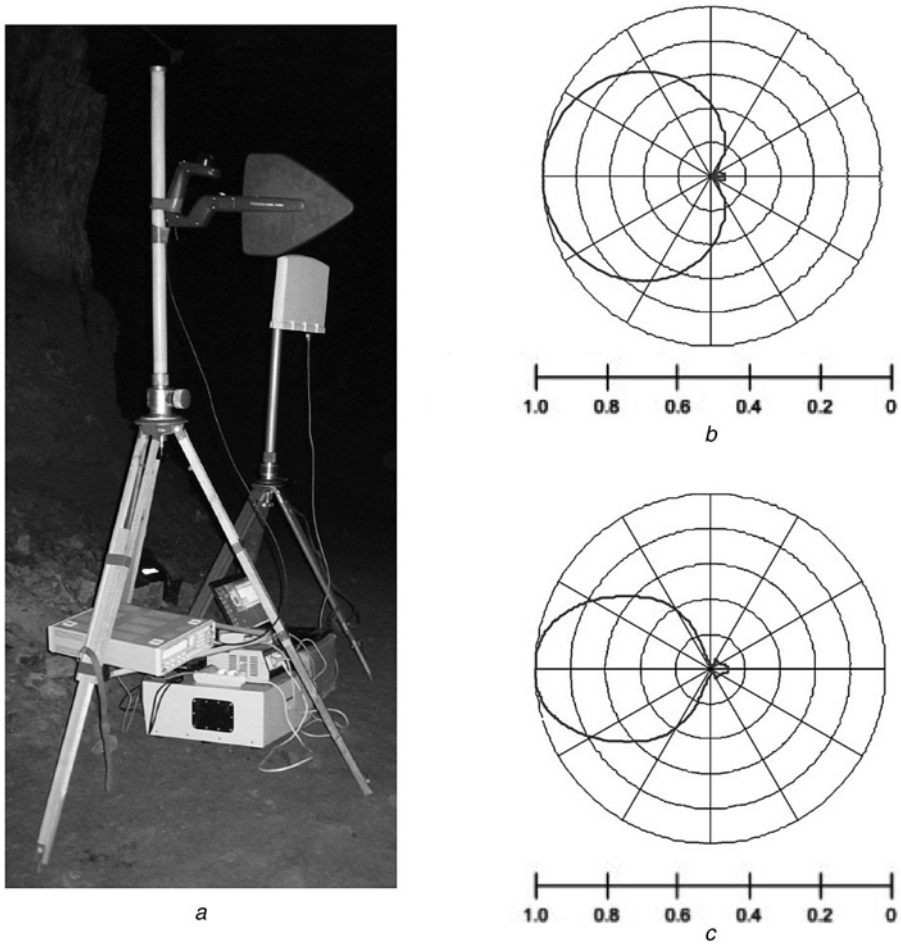

Fig. 6 *Test set located in the mine (a) and the radiation characteristics of the HE300 antenna*

b Horizontal

c Vertical radiation characteristics of the HE300 antenna

During the measurements the 'Max hold' function was set on the spectrum analyser. Therefore for the purpose of the comparative analysis the envelopes of curves obtained during the theoretical calculations were calculated. All simulations were performed for the environment model shown in Fig. 7*b*. For the case described as a 'flat surface' calculations were performed without the developed scattering model. For the case '2D surface model' calculations were performed with implemented (9) and (10) and for the '3D surface model' case with implemented (13) and (14) (Fig. 8).

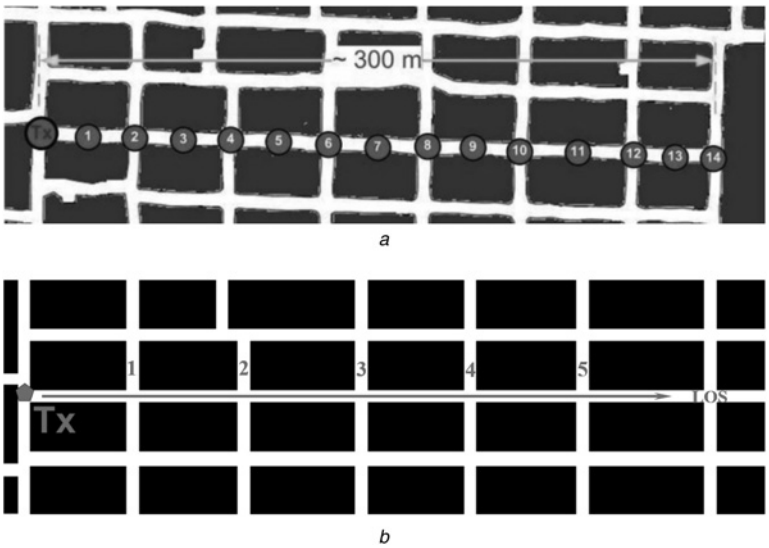

Fig. 7 *Plan of mine corridors with measurements points (a) and a model of mine used in simulation with number of side coridors (b)*

IET Microw. Antennas Propag., 2015, Vol. 9, Iss. 12, pp. 1241–1248

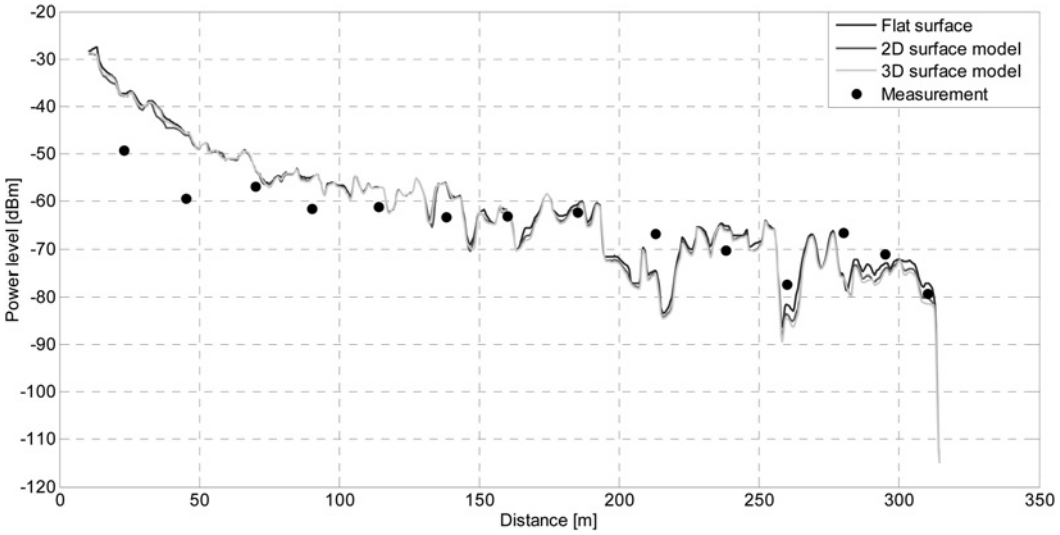

Fig. 8 *Example of comparison of the theoretical results with measurements for 2.4 GHz*

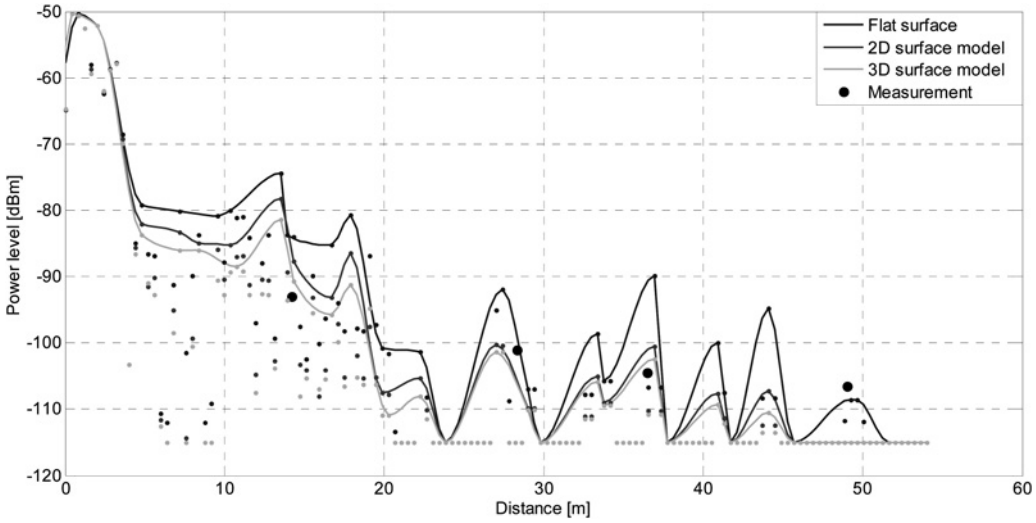

Fig. 9 *Example of comparison theoretical results with measurements for 1.5 GHz for third corridor with NLOS conditions*

As one can see the use of the electromagnetic wave scattering model has no apparent impact on the obtained calculated results in comparison with the flat surfaces for the LOS conditions. This is because the direct component is the most significant for direct visibility. The scattering does not affect the electric field strength value of the direct component, hence the impact of the developed model is small. An analysis of calculation errors in relation to measurement results was carried out for all measurement points in a manner allowing to observe an improvement in the EM field prediction, achieved after including the scattering models to the basic 'flat surface' case.

Table 1 shows the calculation results of absolute error for all measurement frequencies. For each measurement frequency the module of the mean value of absolute error was calculated for the three reflective surfaces according to

$$\Delta P_{\text{mean}} = \frac{\sum_i^n |P_{i\,\text{cal}} - P_{i\,\text{meas}}|}{n} \tag{17}$$

where, $P_{i\text{cal}}$ – calculated power level at point i, $P_{i\text{meas}}$ – measured power level at point i, n – number of measurements points.

Based on the determined error values, the degree of improvement in the accuracy of the signal power prediction in the real indoor environment was determined in relation to the flat surfaces. The value of this degree is defined as the difference in the error determined for the flat surface, and the error calculated for irregular surfaces. It should be noted that the error values were

Table 1 Mean value of absolute error for LOS condition

Frequency	Type of reflecting surface	ΔP_{mean}, dB	$\Delta P_{\text{mean flat}} - \Delta P_{\text{sr 2D(3D)}}$, dB
910 MHz	flat	9.1	–
	2D irregular	8.9	0.2
	3D irregular	8.8	0.2
1510 MHz	flat	8.8	–
	2D irregular	9.0	−0.1
	3D irregular	8.9	−0.1
2440 MHz	flat	5.8	–
	2D irregular	5.6	0.2
	3D irregular	5.8	0.0
mean value for all frequencies	flat	7.9	–
	2D irregular	7.8	0.1
	3D irregular	7.9	0.0

Table 2 Mean value of absolute error for NLOS condition

Frequency	Type of reflecting surface model	ΔP_{mean}, dB	$\Delta P_{mean\ flat} - \Delta P_{mean\ 2D(3D)}$, dB
910 MHz	flat	20.2	–
	2D irregular	15.5	4.7
	3D irregular	10.8	9.4
1510 MHz	flat	10.0	–
	2D irregular	9.3	0.7
	3D irregular	8.8	1.2
2440 MHz	flat	10.1	–
	2D irregular	5.5	4.6
	3D irregular	5.7	4.4
mean value for all frequencies	flat	13.4	–
	2D irregular	10.1	3.3
	3D irregular	8.4	5.0

calculated for the exact value and then were approximated to one decimal place. Therefore the values given in the tables below may have inaccuracies of up to 0.1 dB. The primary conclusion on the basis of the obtained results is that the use of the developed model for LOS conditions does not increase the prediction accuracy.

In the next step, investigations similar to those along the main passage were also carried out for transverse corridors, obviously under NLOS conditions. Respective measurements and simulations were performed for corridors shown in Fig. 7*b*. Owing to the symmetry with respect to the main corridor, measurements were made only in the corridors lying on one side of this corridor, assuming that for the other side the electromagnetic field distribution is approximately the same. It should be noted that because of the low power levels that occur in the transverse passage ways and the ability of the measuring equipment, the measurements were carried out at points where the measured power were greater than around −110 dBm. Therefore in the calculation the lower power threshold was set at −115 dBm.

Fig. 9 illustrates an example of comparative results of calculations and measurements for the NLOS conditions. As can be seen, now the differences between outcomes attained for the flat-surface case and the irregular-surface cases (both 2D and 3D) are far more pronounced than in the LOS case (compare with Fig. 9) at 2.4 GHz. As for the remaining frequencies, respective outcomes were presented in Table 2 indicating an improvement of up to 10 dB in the EM field prediction accuracy relative to measurements. These values have been calculated analogously to the LOS conditions in accordance with the relation (17).

5 Summary

On the basis of the results it can be concluded that the use of the presented scattering models increases notably the accuracy of the electromagnetic field prediction in the mine environment for NLOS conditions only. In turn, their use in LOS conditions proves insignificant in terms of affecting the accuracy of the electromagnetic field because of the overwhelming the presence of the dominant direct ray.

An additional important finding is that the use of these developed scattering models does not basically affect the simulation time which depends mainly on the environment complexity, which was the same throughout all simulations. In all investigated scenarios of walls irregularities (i.e. without the scattering models and including the 2D and 3D models), the simulation time was almost identical.

Finally, it could be noted that better results are obtained using the 3D surface scattering model owing to the fact that this model more realistically represents the distribution of irregularity heights of real walls surfaces encountered in mines.

6 References

1 Jian, Y.L., Yerong, Z., Wei, C.: 'A novel approach for radio propagation in indoor environment'. Int. Conf. on Microwave and Millimeter Wave Technology, 2008, vol. 4, pp. 1910–1912
2 Rautiainen, T., Hoppe, R., Wolfle, G.: 'Measurements and 3D ray tracing propagation predictions of channel characteristics in indoor environments'. IEEE 18th Int. Symp. on Personal, Indoor and Mobile Radio Communications, 2007, pp. 1–5
3 Mani, F., Oestges, C.: 'Evaluation of diffuse scattering contribution for delay spread and crosspolarization ratio prediction in an indoor scenario'. Proc. of the Fourth European Conf. on Antennas and Propagation, 2010, pp. 1–4
4 Azpilicueta, L.: 'Characterization of wireless propagation in complex indoor scenarios'. IEEE 14th Int. Symp. and Workshops on a World of Wireless, Mobile and Multimedia Networks, 2013, pp. 1–2
5 Cheng, E.M., Abbas, Z., Fareq, M., *et al.*: 'Comparative study between measurement and predictions using geometrical optics and uniform theory of diffraction for case of non-line-of-sight in indoor environment' (Springer Science Business Media, New York, 2012)
6 Li, M., Zhou, L., Zheng, Z.: 'Analysis of electromagnetic wave propagation characteristics in rectangular tunnels based on the geometrical optics method'. Int. Conf. on Microwave and Millimeter Wave Technology (ICMMT), 2012, vol. 2, pp. 1–3
7 Shan-Hua, Y., Xian-Liang, W.: 'Electromagnetic waves multi-path model based on image approach in tunnels'. Int. Conf. on Electric Information and Control Engineering, 2011, pp. 2150–2153
8 Kishiki, Y., Takada, J., Ching, G.S., *et al.*: 'Application of reflection on curved surfaces and roughness on surface in ray tracing for tunnel propagation'. Proc. of the Fourth European Conf. on Antennas and Propagation, 2010, pp. 1–5
9 Fuschini, F., Falciasecca, G.: 'A mixed rays – modes approach to the propagation in real road and railway tunnels', *IEEE Trans. Antennas Propag.*, 2012, **60**, (2), pp. 1095–1105
10 Liu, C.G., Zhang, E.T., Wu, Z.P., Zhang, B.: 'Modelling radio wave propagation in tunnels with ray-tracing method'. Seventh European Conf. on Antennas and Propagation, 2013, pp. 2317–2321
11 Emslie, A., Lagace, R., Strong, P.: 'Theory of the propagation of UHF radio waves in coal mine tunnels', *IEEE Trans. Antennas Propag.*, 1975, **23**, (2), pp. 192–205
12 Subrt, L., Pechac, P.: 'Semi-deterministic propagation model for subterranean galleries and tunnels', *IEEE Trans. Antennas Propag.,* 2010, **58**, (11), pp. 3701–3706
13 Staniec, K.: 'Modeling the influence of walls shapes on radio signal properties in mines'. Antennas and Propagation Society Int. Symp., 2009. APSURSI '09. IEEE, 1–5 June 2009, pp. 1–4
14 Gentile, C., Valoit, F., Moayeri, N.: 'A ray tracing model for wireless propagation in tunnels with varying cross section'. Global Communications Conf. IEEE, 2012, pp. 5027–5032
15 Choudhury, B., Jha, R.M.: 'A refined ray tracing approach for wireless communications inside underground mines and metrorail tunnels'. IEEE Applied Electromagnetics Conf., 2011, pp. 1–4
16 Xu, Z., Huo, Y., Zheng, H.D.: 'The effect of the wall roughness on the electromagnetic wave propagation in coal mine underground'. IEEE Int. Symp. on Knowledge Acquisition and Modeling Workshop, 2008, pp. 482–485
17 Shan-hua, Y.: 'Analysis on the characteristics of electromagnetic wave scattering on mine tunnels wall'. Third Int. Congress on Image and Signal Processing, 2010, vol. 9, pp. 4354–4357
18 Forooshani, A., Bashir, S., Michelson, D., Noghanian, S.: 'A survey of wireless communications and propagation modeling in underground mines'. Communications Surveys and Tutorials, IEEE, vol. 99, pp. 1524–1545
19 Ndoh, M., Delisle, G.Y.: 'Underground mines wireless propagation modeling'. VTC2004-Fall. 2004 IEEE 60th, 2004, vol. 5, pp. 3584–3588
20 Sun, Z., Akyildiz, I.: 'Channel modeling and analysis for wireless networks in underground mines and road tunnels', *IEEE Trans. Commun.*, 2010, **58**, pp. 1758–1768
21 Boutin, S., Affes, M., Despin, C., Denidni, T.: 'Statistical modeling of a radio propagation channel in an underground mine at 2.4 and 5.8 GHz'. Proc. IEEE VTC, 2005, vol. 1, pp. 78–81
22 www.siradel.com
23 http://www.awe-communications.com/
24 Ulaby, F., Moore, R., Fung, A.: 'Microwave remote sensing active and passive', in 'Radar remote sensing and surface scattering and emission theory' (Addison-Wesley Publishing Company, 1982), vol. 2
25 Kubal, S., Kowal, M., Piotrowski, P., Zielinski, R.J.: 'Irregular surfaces modelling for propagation analysis in the complex indoor environment'. Int. Symp. on Electromagnetic Compatibility, 2014, pp. 985–990
26 Katulski, R.: 'Propagacja fa radiowych' (in Polish) (WKŁ Warszawa, 2009), pp. 213–223
27 Rappaport, T.S.: 'Wireless communications: principles and practice (2nd edition)' (Prentice Hall, 2002), ISBN 978-0130422323, p. 80
28 Recommendation ITU-R P.527-3 – Electrical characteristics of the surface of the Earth
29 Vaughan, R., Andersen, J.B.: 'Channels, propagation and antennas for mobile communications' (The Institution of Electrical Engineers, 2003)